

## Research Paper

# Preparation and Luminescence of Europium-doped Yttrium Oxide Thin Films

Myun Hwa Chung and Joo Han Kim\*

Department of Advanced Materials Engineering Chungbuk National University, Cheongju 28644, Korea

Received February 28, 2017; revised March 27, 2017; accepted March 27, 2017

**Abstract** Thin films of europium-doped yttrium oxide ( $\text{Y}_2\text{O}_3:\text{Eu}$ ) were prepared on Si (100) substrates by using a radio frequency (RF) magnetron sputtering. After the deposition, the films were annealed at  $1000^\circ\text{C}$  in an air ambient for 1 hour. X-ray diffraction analysis revealed that the  $\text{Y}_2\text{O}_3:\text{Eu}$  films had a polycrystalline cubic  $\alpha\text{-Y}_2\text{O}_3$  structure. The as-deposited films showed no photoluminescence (PL), which was due to poor crystalline quality of the films. The crystallinity of the  $\text{Y}_2\text{O}_3:\text{Eu}$  films was significantly improved by annealing. The strong red PL emission was observed from the annealed  $\text{Y}_2\text{O}_3:\text{Eu}$  films and the highest intensity peak was centered at around 613 nm. This emission peak originated from the  $^5\text{D}_0 \rightarrow ^7\text{F}_2$  transition of the trivalent Eu ions occupying the  $\text{C}_2$  sites in the cubic  $\alpha\text{-Y}_2\text{O}_3$  lattice. The broad PL excitation band was observed at wavelengths below 280 nm, which was attributed to the charge transfer transition of the trivalent Eu ion.

**Keywords:** Yttrium Oxide, Rare Earth Element, Sputtering, Luminescence

## I. Introduction

Yttrium oxide ( $\text{Y}_2\text{O}_3$ ) has received considerable attention because it possesses many special properties, such as high melting point (over  $2400^\circ\text{C}$ ), high dielectric constant (15), high thermal conductivity ( $27 \text{ W m}^{-1} \text{ K}^{-1}$  at 300 K), large bandgap (5.6 eV), high refractive index ( $\sim 1.9$ ), and high mechanical strength [1,2].  $\text{Y}_2\text{O}_3$  has been extensively used for a wide variety of applications from traditional refractories to advanced ceramic technologies.  $\text{Y}_2\text{O}_3$  has also become an important material for optical applications because of its ability to be a host material for rare earth elements. Especially, europium (Eu)-doped  $\text{Y}_2\text{O}_3$  shows an efficient red emission, which makes it suitable to be used as a red-emitting phosphor material [3-5].

$\text{Y}_2\text{O}_3:\text{Eu}$  has been synthesized in powder form by using a number of different methods, including solution combustion [3], hydrothermal [4], co-precipitation [6], solid state reaction [7], sol gel [8], and spray pyrolysis [9] techniques. Compared to the powder form,  $\text{Y}_2\text{O}_3:\text{Eu}$  in thin-film form could offer several advantages, such as better thermal stability, good adhesion to the substrate surface, higher resolution, and uniform properties across the covered area [10]. However, in spite of these potential advantages, relatively little work has so far been carried out on the thin-film form of  $\text{Y}_2\text{O}_3:\text{Eu}$ . In this study,  $\text{Y}_2\text{O}_3:\text{Eu}$  thin films

were prepared by using a radio frequency (RF) magnetron sputtering. The crystalline structure, photoluminescence emission and excitation characteristics of the prepared films were investigated.

## II. Experiments

The  $\text{Y}_2\text{O}_3:\text{Eu}$  thin films were prepared by RF magnetron sputtering from an Eu-doped  $\text{Y}_2\text{O}_3$  target under an argon gas atmosphere. A schematic diagram of the sputtering chamber is illustrated in Fig. 1. The p-type Si (100)-oriented wafers were used as substrates. The sputtering chamber was pumped to a base pressure of less than  $1 \times 10^{-6}$  Torr. The RF power density and gas pressure were kept constant at  $5.92 \text{ W cm}^{-2}$  and 20 mTorr, respectively,

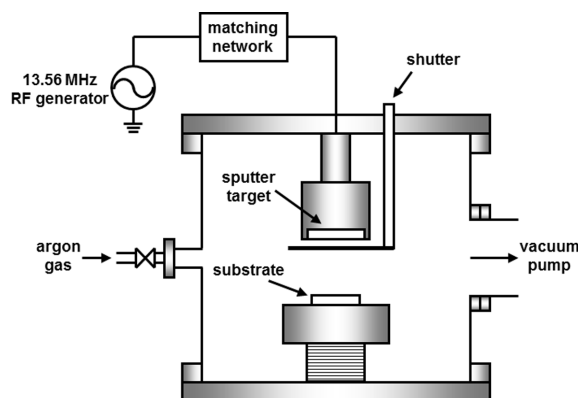


Figure 1. Schematic diagram of the RF magnetron sputtering chamber.

\*Corresponding author  
E-mail: joohan@cbnu.ac.kr

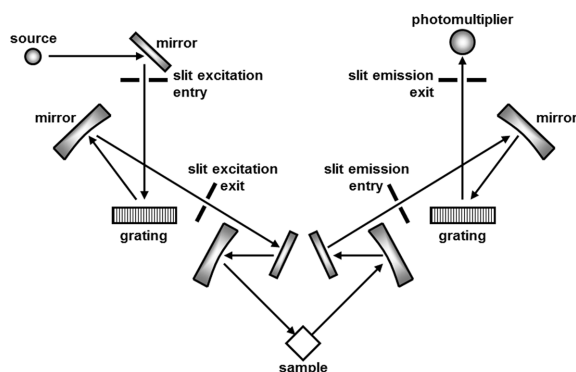


Figure 2. Schematic view of the setup for the photoluminescence measurements.

throughout the deposition. The Si substrates were not intentionally heated during the deposition of the films. The deposited  $\text{Y}_2\text{O}_3:\text{Eu}$  films were then post-annealed at  $1000^\circ\text{C}$  for 1 hour in air ambient. The crystalline structure of the films was examined by X-ray diffraction (XRD) analysis using a Bruker D8 Discover diffractometer. The surface morphology was analyzed by using a Carl Zeiss field emission scanning electron microscope (SEM). The elemental composition of the films was measured using an energy-dispersive X-ray (EDX) analysis. The photoluminescence excitation and emission spectra were collected at room temperature over the wavelength range from 200 to 800 nm with a resolution of 0.5 nm. A schematic view of the setup for the photoluminescence measurements is depicted in Fig. 2.

### III. Results and Discussion

Figure 3 shows a typical EDX spectrum obtained from the  $\text{Y}_2\text{O}_3:\text{Eu}$  films. The Si peak originates from the Si wafer substrate. The Eu concentration was determined to be approximately 1 at.%. Figure 4 presents a typical SEM image of the  $\text{Y}_2\text{O}_3:\text{Eu}$  films. It can be seen from Fig. 4 that the  $\text{Y}_2\text{O}_3:\text{Eu}$  film is very uniform and free from any porosity. No particulates are visible on the film surface. From the mapping micrograph of Eu element of this sample, as shown in Fig. 5, it can be found that Eu element is homogeneously distributed throughout the film.

The XRD patterns for the as-deposited and the post-annealed  $\text{Y}_2\text{O}_3:\text{Eu}$  films are given in Figs. 6(a) and 6(b), respectively. The as-deposited films exhibit a relatively

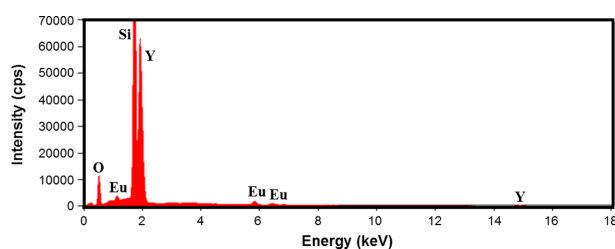


Figure 3. EDX spectrum obtained from the  $\text{Y}_2\text{O}_3:\text{Eu}$  films deposited on the Si substrate.

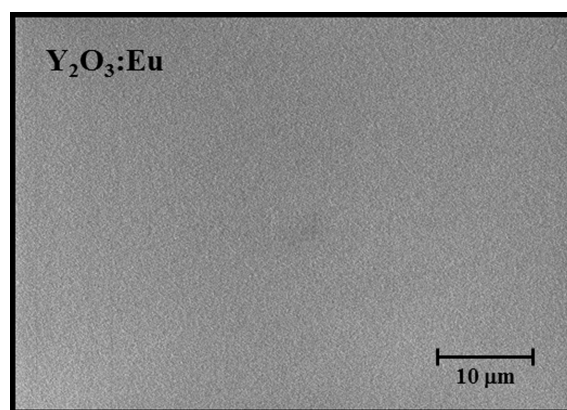


Figure 4. SEM micrograph showing the surface of the  $\text{Y}_2\text{O}_3:\text{Eu}$  films.

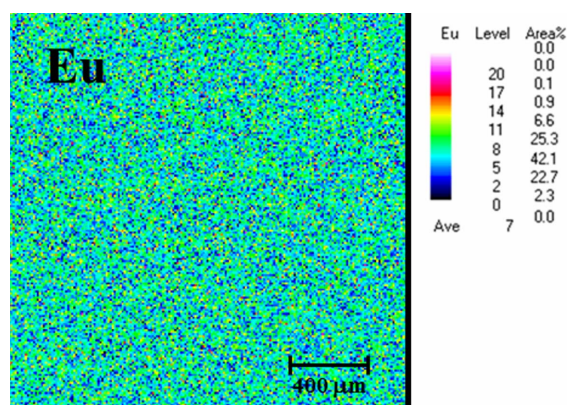


Figure 5. Mapping micrograph of Eu element of the  $\text{Y}_2\text{O}_3:\text{Eu}$  films.

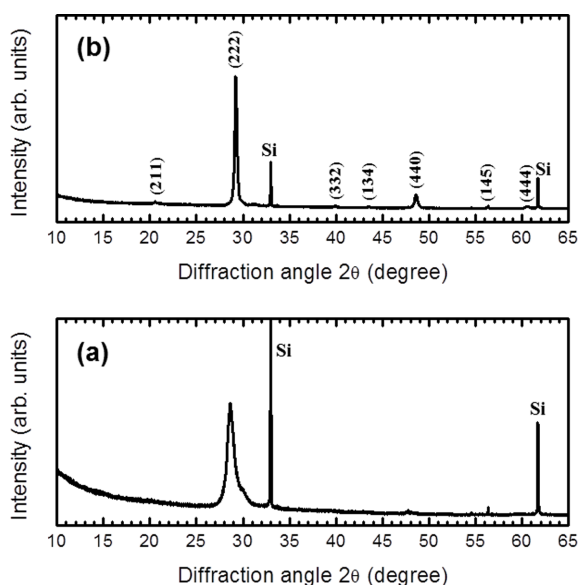
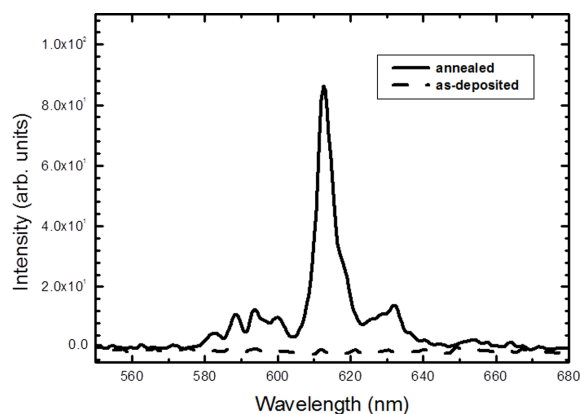


Figure 6. XRD patterns of the  $\text{Y}_2\text{O}_3:\text{Eu}$  films (a) as-deposited and (b) annealed at  $1000^\circ\text{C}$  for 1 hour.

weak and broad peak, indicating the poor crystalline quality of the films. The diffraction peaks from the annealed films are much stronger and sharper than those from the as-deposited films, revealing that the crystallinity was significantly improved by annealing. All the positions



**Figure 7.** Photoluminescence emission spectra of the  $\text{Y}_2\text{O}_3\text{:Eu}$  films.

of the diffraction peaks, except the Si substrate peaks, correspond to diffraction lines in the cubic-crystal-structured  $\alpha\text{-Y}_2\text{O}_3$  phase [11]. The lattice parameter of the  $\alpha\text{-Y}_2\text{O}_3$  crystallites in the annealed films can be determined by using the formula for cubic crystal structure [12],

$$\frac{1}{d_{hkl}^2} = \frac{h^2 + k^2 + l^2}{a^2},$$

where  $a$  is the lattice parameter and  $d_{hkl}$  is the spacing between the  $(hkl)$  planes. The lattice parameter thus computed is  $a = 10.58 \text{ \AA}$ , which is in reasonable agreement with that given in the JCPDS database [11].

Figure 7 presents the photoluminescence emission spectra of the as-deposited and annealed  $\text{Y}_2\text{O}_3\text{:Eu}$  films. No luminescence was observed from the as-deposited films and this is considered to be due to the poor crystalline quality of the films, as verified by XRD analysis. The strong PL emission was observed from the annealed  $\text{Y}_2\text{O}_3\text{:Eu}$  films and the spectrum was composed of a group of peaks. The small peak centered at 582 nm originates from the  $^5\text{D}_0 \rightarrow ^7\text{F}_0$  transition of the trivalent Eu ions. The three peaks at 588, 594, and 600 nm are from the  $^5\text{D}_0 \rightarrow ^7\text{F}_1$  transition. The intense red emission peak at 613 nm and a small peak at 632 nm are from the  $^5\text{D}_0 \rightarrow ^7\text{F}_2$  transition.

It should be noted that the emission intensity from the  $^5\text{D}_0 \rightarrow ^7\text{F}_2$  transition is much stronger than that from the  $^5\text{D}_0 \rightarrow ^7\text{F}_1$  transition. It has been reported that the intensity of the  $^5\text{D}_0 \rightarrow ^7\text{F}_2$  transition is strongly dependent upon changes in local symmetry environment around the trivalent Eu ion [13]. However, the  $^5\text{D}_0 \rightarrow ^7\text{F}_1$  intensity is relatively unaffected by this local environment because of its pure magnetic dipole character. Therefore, the intensity ratio of  $^5\text{D}_0 \rightarrow ^7\text{F}_2$  to  $^5\text{D}_0 \rightarrow ^7\text{F}_1$  is usually regarded as a measure of inversion symmetry of the trivalent Eu site in the host lattice. It is thus expected that the higher this ratio, the lower the trivalent Eu site symmetry. This ratio is determined to be approximately 6.84 for the  $\text{Y}_2\text{O}_3\text{:Eu}$  films prepared in this study. This high value of the ratio suggests that the trivalent Eu ion is less likely to occupy a site with inversion symmetry. As already confirmed in the above

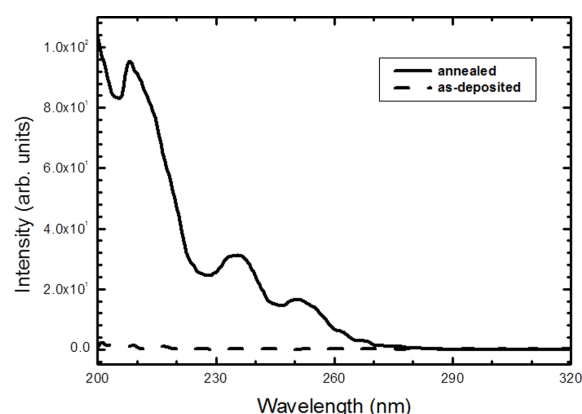


**Figure 8.** PL excitation spectra measured from the  $\text{Y}_2\text{O}_3\text{:Eu}$  films.

XRD analysis, the  $\text{Y}_2\text{O}_3\text{:Eu}$  films consist of cubic  $\alpha\text{-Y}_2\text{O}_3$  crystallites. The cubic  $\alpha\text{-Y}_2\text{O}_3$  structure has a space group  $T_h^{7-}$  symmetry with two different crystallographic sites, i.e.,  $\text{C}_2$  and  $\text{S}_6$  sites [14]. The  $\text{C}_2$  site has relatively poor inversion symmetry, but the  $\text{S}_6$  site has perfect inversion symmetry. It can therefore be found that the trivalent Eu ions occupy mainly the  $\text{C}_2$  sites in cubic  $\alpha\text{-Y}_2\text{O}_3$  lattice, resulting in the high luminescence intensity of the  $^5\text{D}_0 \rightarrow ^7\text{F}_2$  transition. Figure 8 shows the PL excitation spectra measured from the  $\text{Y}_2\text{O}_3\text{:Eu}$  films. The broad PL excitation band was observed from the annealed films at wavelengths below 280 nm. This is attributed to the charge transfer transition of the trivalent Eu ion, which is typical of  $\text{Eu}^{3+}$ -activated metal oxide phosphors [5].

#### IV. Conclusions

Thin films of  $\text{Y}_2\text{O}_3\text{:Eu}$  were prepared by using an RF magnetron sputtering and their structure and luminescence were investigated. The  $\text{Y}_2\text{O}_3\text{:Eu}$  films exhibited a polycrystalline cubic  $\alpha\text{-Y}_2\text{O}_3$  structure. No peak could be recognized in the PL emission and excitation spectra measured from the as-deposited  $\text{Y}_2\text{O}_3\text{:Eu}$  films, which is considered to be due to the poor crystalline quality of the films. A significant improvement of the crystallinity of the films was achieved by annealing at  $1000^\circ\text{C}$  for 1 hour in air. The intense PL emission peaked at around 613 nm in the red range was observed from the annealed films, resulting from the hypersensitive transition between the  $^5\text{D}_0$  and  $^7\text{F}_2$  levels of the trivalent Eu ions. The broad PL excitation spectrum was obtained at wavelengths below 280 nm, which was accounted for by the charge transfer transition of the trivalent Eu ion.

#### Acknowledgments

This work was supported by the Basic Science Research Program through the National Research Foundation (NRF) of Korea funded by the Ministry of Education (2013R1A1A2013617). This work was also supported by a research

grant from the Chungbuk National University in 2014.

## References

- [1] A. Fukabori, T. Yanagida, J. Pejchal, S. Maeo, Y. Yokota, A. Yoshikawa, T. Ikegami, F. Moretti, and K. Kamada, *J. Appl. Phys.* 107, 073501 (2010).
- [2] G. D. Wilk, R. M. Wallace, and J. M. Anthony, *J. Appl. Phys.* 89, 5243 (2001).
- [3] Y.-P. Fu, S.-B. Wen, and C.-S. Hsu, *J. Alloys Comp.* 458, 318 (2008).
- [4] G. Chen, W. Qi, Y. Li, C. Yang, and X. Zhao, *J. Mater. Sci.: Mater. Electron.* 27, 5628 (2016).
- [5] G. Blasse and B. C. Grabmaier, *Luminescent Materials* (Springer-Verlag, Berlin, Heidelberg, 1994).
- [6] X. Wu, Y. Liang, R. Liu, and Y. Li, *Mater. Res. Bull.* 45, 594 (2010).
- [7] L. Ma, X. Hu, S. Sun, J. Liu, J. Hu, and S. Yan, *J. Electrochem. Soc.* 156, P39 (2009).
- [8] V. B. Taxak, S. P. Khatkar, S.-D. Han, R. Kumar, and M. Kumar, *J. Alloys Comp.* 469, 224 (2009).
- [9] Y. Shimomura and N. Kijima, *Electrochem. Solid-State Lett.* 7, H1 (2004).
- [10] Y. Nakanishi, A. Miyake, H. Kominami, T. Aoki, Y. Hatanaka, and G. Shimaoka, *Appl. Surf. Sci.* 142, 233 (1999).
- [11] Joint Committee on Powder Diffraction Standards (JCPDS), Powder Diffraction Files, Inorganic, No. 43-1036.
- [12] B. D. Cullity, *Elements of X-ray Diffraction*, 2nd ed. (Addison-Wesley, Reading, MA, 1978).
- [13] L. Liu, R. Li, Y. Deng, L. Li, S. Lan, W. Zi, and S. Gan, *Appl. Surf. Sci.* 307, 393 (2014).
- [14] M. Buijs, A. Meyerink, and G. Blasse, *J. Lumin.* 37, 9 (1987).